05,10

Synthesis and physical properties of Fe−Ni alloy nanowires in alumina matrices of different morphologies

© A.E. Dryagina[1], A.N. Gorkovenko[1], A.A. Veryasova[1], A.A. Ushkov[1], E.V. Kudyukov[1], N.A. Kulesh[?], V.O. Vas'kovskiy[1,2]

[1] Ural Federal University after the first President of Russia B.N. Yeltsin, Yekaterinburg, Russia
[2] M.N. Mikheev Institute of Metal Physics, Ural Branch, Russian Academy of Sciences, Yekaterinburg, Russia

E-mail: anastasia.dryagina@urfu.ru, a.n.gorkovenko@urfu.ru, alenaver75@gmail.com

Received March 6, 2025
Revised March 6, 2025
Accepted May 5, 2025

In this work, a comparative study of the microstructure, magnetic and magnetoresistive properties of arrays of Fe−Ni nanowires with different morphologies has been carried out. They were obtained by electrolytic metal deposition in porous alumina matrices prepared by different, including original, techniques. All nanowires samples are polycrystalline and have a face-centred cubic lattice. The relationship between the remagnetisation properties and the morphology of the nanowire arrays was revealed. The presence of the magnetoresistance anisotropy effect was found, the magnitude of which was 1.3−2.3 % for samples of different types.

Keywords: anodisation, alumina, porous matrix, electrolytic deposition, nanowires, magnetic properties, magnetoresistance.

DOI: 10.61011/PSS.2025.07.61884.3HH-25

1. Introduction

Magnetic nanowires (NWs) are an interesting class of magnetic nanomaterials, since due to their geometry and dimensional characteristics they demonstrate properties promising for use in various technical fields, including media for high-density information recording, spintronics devices, highly sensitive sensors and microwave technology components [1–6]. In particular, NWs can be used to create magnetoresistive sensor elements with a high level of basic electrical resistance.

In addition to the starting material, the magnetic and resistive properties of both arrays and individual nanowires directly depend on the shape, size, and packing density of the nanowires in the matrix. The possibility of variation of these parameters is largely determined by the technology of NWs synthesis. In this regard, one of the most effective methods for obtaining nanowire arrays is the electrodeposition of ferromagnetic metal into anodic aluminium oxide (AAO) matrices [7]. Using AAO as templates for NWs makes it possible to obtain arrays of ordered nanowires with high density and adjustable geometric parameters [7], which is important for an adequate analysis of the properties of the studied objects and possible practical applications.

The traditional synthesis technique involves removal of aluminum from the back of the AAO and application of a conductive metal layer (Ti,Cu,Au), which serves as a contact for electrochemical deposition [5–8]. However, in this paper, an alternative approach is proposed, which consists in using a non-oxidized aluminum base AAO as a conductive substrate, which somewhat simplifies the synthesis process. This method eliminates the stage of chemical removal of aluminum, reducing the risk of damage to the matrix and provides the potential for reuse of aluminum.

Along with the magnetism of NWs, their resistive properties are of considerable interest, which are realized, among other things, when a spin-polarized current is passed through NWs. The latter is relevant in connection with research into the prospects for electrical control of the magnetic state of systems [6,9]. In addition, an electric current can be applied to the domain walls and domains inside the nanowires, which also makes it possible to control their magnetic state [10–14]. All this characterizes NWs as a separate type of magnetic materials that can find appropriate functional applications in the development of new generations of magnetic, spintronic, and neuromorphic devices [15–18].

Despite significant progress, unexplored aspects remain. In particular, the effect of anisotropic magnetoresistance (AMR) has been studied for single Ni and Co nanowires [19–22], but has not been demonstrated for arrays of NWs made of Fe−Ni alloy. In addition, on this side, NWs with a branched structure were not considered, although their morphology can significantly affect their properties.

The main objective of this work was a comparative study of the microstructure, magnetic and magnetoresistive properties of NWs arrays of Fe−Ni alloy with different morphologies of individual elements, the implementation of which is based on the application of classical and original methods of electrolytic synthesis of the corresponding

objects, including those with surface electrically conductive layers.

2. Experimental methodology

2.1. Materials and equipment

The following equipment was used for the synthesis of porous aluminum oxide matrices and the electrodeposition of nanowires: DC power source AKIP-1133-300-2.5 (JSC „PriST“, Russia), chiller DLK-2003 (LLC „Vilitek“, Russia), original fluoroplast chemical cell.

Electrolytes for anodizing and electrodeposition were mixed from the following materials: oxalic acid (chemically pure) $C_2H_2O_4 \cdot 2H_2O$, GOST 22180-76 (JSC „VEKTON“); iron sulfate (chemically pure) $FeSO_4 \cdot 7H_2O$, GOST 4148-78 with amendments 1, 2 (LLC „Raspberry Lake Trading House“); nickel sulfate (chemically pure) $NiSO_4 \cdot 7H_2O$, GOST 4465-2016 (JSC „VEKTON“); boric acid (chemically pure) H_3BO_3, GOST 9656-75 with amendments 1, 2, 3 (LLC „KhimTrast“); copper sulfate $CuSO_4 \cdot 5H_2O$, GOST 19347-99, grade A, first grade (Russia).

For etching aluminum, a solution of hydrochloric acid (chemically pure) HCl, GOST 3118-77 with modification 1 (JSC„Kaustic“) and copper chloride (II) (chemically pure) $CuCl_2 \cdot 2H_2O$, GOST 4167-74 with amendments 1 (LLC „Reakhim“), as well as an aqueous solution of orthophosphoric acid (UHP) H_3PO_4, TU 2612-014-00203677-97 (JSC „Rheatex“) and a solution of orthophosphoric acid with chromium oxide, GOST 3776-78 with amendments 1, 2 (AO „Russian Chromium 1915“).

To dissolve the oxide matrix, a solution of sodium hydroxide (chemically pure) NaOH, GOST 4328-77 (LLC „OTK“) was used.

A neodymium magnet N38 $0.01 \times 0.005 \times 0.002$ m (China) was used to assemble the nanowires.

The morphology, structure, and composition of the NWs arrays were studied using a transmission electron microscope JEOL-2100. Magnetometric hysteresis loops were obtained using a Lake Shore 7407 vibrating magnetometer at room temperature in the field range ± 15 kOe when an external magnetic field was applied along and perpendicular to the axis of the nanowire array. The measurement of the magnetoresistive properties was carried out on the original magnetoresistive installation using a pseudo-four-probe method. The measuring unit consisted of an electromagnet, two universal voltmeters AKIP-V7-78/1 for measuring voltage and current, as well as a direct current source. The value of the direct current flowing through the sample was 0.61 mA. The data was recorded and processed using an original visual program in the LabVIEW programming environment. The measurement results were magnetoresistive hysteresis loops $R(H)$, which were obtained by applying an external magnetic field along and perpendicular to the axis of the nanowire array (axis perpendicular to the plane of the AAO template) at room temperature in the field range ± 8 Oe.

2.2. Synthesis of nanowires

Within the framework of this study, three types of nanowire arrays were obtained: *A*, *B* and *C*. The synthesis of each type was carried out in two main stages: the formation of a porous aluminum oxide template and its subsequent filling with magnetic material by electrolytic deposition. The main differences between the samples of different types were in the features of their morphology, which were a consequence of the specifics of the methods of formation of oxide matrices at the first stage of synthesis. For greater clarity, Figure 1 shows a schematic representation of the processes of manufacturing different types of AAO templates.

High-purity aluminum foil with a thickness of ~ 1 mm was used as the starting material. To form a porous aluminum oxide matrix, a two-stage anodizing method was used in an aqueous solution of oxalic acid (with a concentration of 3 M), which was carried out on an original installation that included a chemical cell, a direct current source and a chiller to maintain a certain substrate temperature. Aluminum foil served as the anode, and a platinum grid served as the cathode. The anodizing process was carried out at a voltage of 40 V at room temperature. After the first stage of anodizing, which lasted 60 min, the formed aluminum oxide layer was removed in a 7 % aqueous solution of orthophosphoric acid with chromium oxide (with a concentration of 0.18 M). Then the second stage of anodizing was carried out with a duration of 100 min (Figure 1). The use of a two-stage anodizing technique is advisable to form a more ordered array of pores in the aluminum oxide layer [7].

Later, depending on the type of sample, different operations were performed to synthesize different types of AAO templates. Thus, for samples of type *A*, the anodizing process was completed, after which the remaining non-oxidized aluminum was removed from the back of the oxide matrix by chemical etching in an aqueous solution of hydrochloric acid and copper chloride (IV). Then, the barrier layer of aluminum oxide formed at the bottom of the pores during anodizing was removed in a 5 % solution of orthophosphoric acid. As a result, a continuous porous aluminum oxide matrix was obtained. At the next stage, a 200 nm thick layer of copper was deposited on one side of the template by magnetron sputtering, which served as one of the electrodes for subsequent electrolytic deposition of nanowires. Patterns like *A* can be called classical, as they are described in sufficient detail in the literature on the synthesis of arrays of NWs [7,23–27].

In the manufacture of templates of the type *B*, after the main stage of anodizing, the method of stepwise reduction of current and voltage was used to thin the barrier layer [7,28]. The process was carried out during ~ 20 min and ended when the voltage reached $2-3$ V.

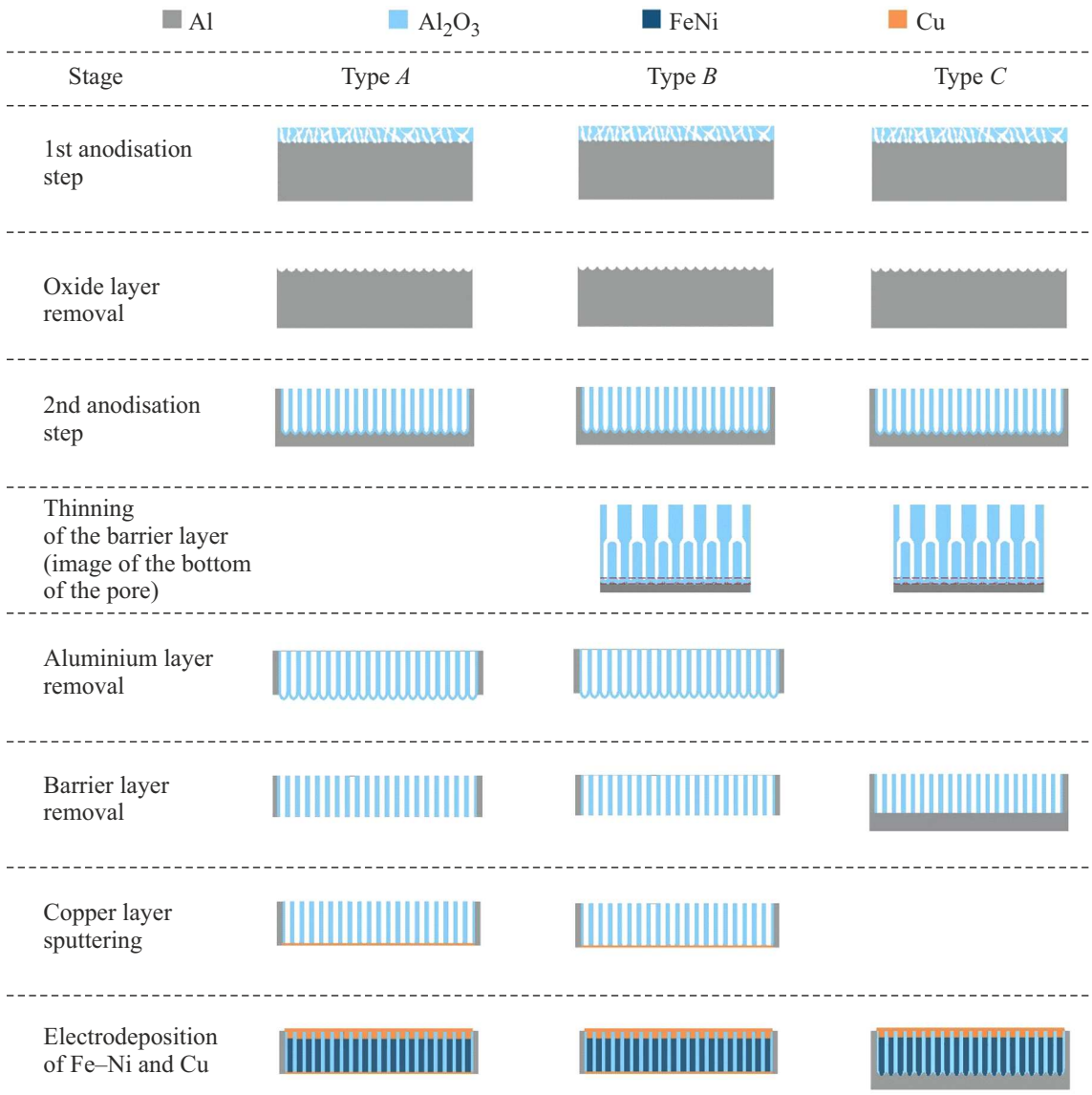

Figure 1. Schematic representation of the main stages of manufacturing arrays of nanowires such as *A, B* and *C*.

Then, similarly to the *A* type templates, the remaining non-oxidized aluminum and the barrier layer at the bottom of the pores were removed, followed by the deposition of a layer of copper.

A distinctive feature of the *C* type templates from others was the removal of the barrier layer at the bottom of the pores without bleaching the remaining non-oxidized aluminum. The following operations were used to achieve this: firstly, a stepwise reduction of current and then voltage after the main stage of anodizing until the values of 0.5 V were reached; secondly, exposure in 5 % solution of orthophosphoric acid was carried out for 70–100 min. As a result, AAO templates with open through-the-hole pores were obtained, providing direct access to metallic aluminum. A clear advantage of manufacturing a template using the method described above is the absence of some labor-intensive technological operations (dissolution of non-oxidized aluminum, deposition of a conductive layer), compared with templates such as *A* and *B*.

The electrolytic deposition of Fe–Ni alloy into various types of aluminum oxide templates was performed at the next stage of the synthesis of NWs arrays. The cathode was a sputtered Cu layer (templates like *A* and *B*) or non-oxidized aluminum (templates like *C*), the anode was a platinum grid. Electrolytic deposition of NWs alloy Fe–Ni was carried out for 7 min from an aqueous solution containing iron sulfate and nickel sulfate, with the addition of boric acid, at room temperature and voltage of 2.5 V (type *A* and *B*) and 4 V (type *C*). Then, the pores were filled by electrolytic deposition of copper from an aqueous solution of copper sulfate, that is, the pores were filled with Cu and released onto the surface of the template, resulting in the formation of a thin conductive film (Figure 1). This

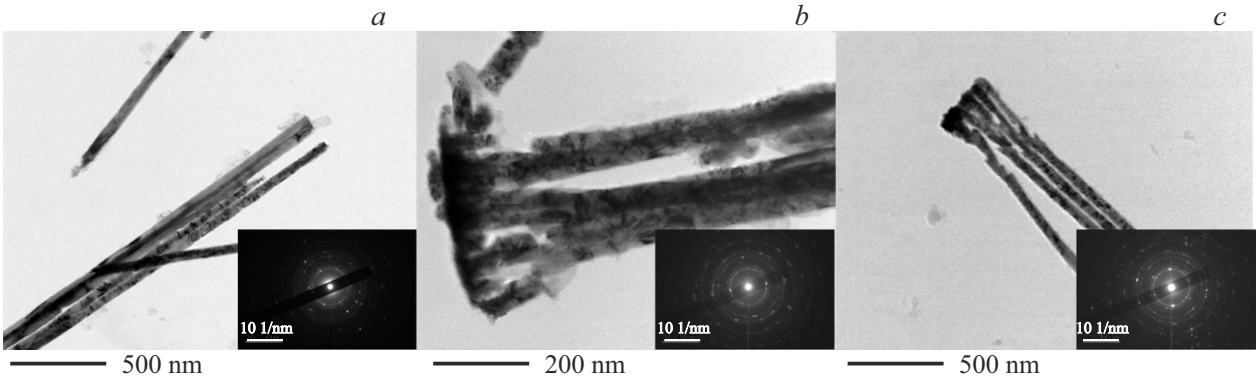

Figure 2. TEM images of NWs types A (a), B (b) and C (c), obtained using a transmission electron microscope. The corresponding electron diffraction patterns are shown in the inserts.

was necessary to obtain an electrical contact on the upper end surface of the NWs array.

Thus, arrays of Fe−Ni alloy nanowires of three types were obtained in this study that differ in morphology, due to the peculiarities of production of the corresponding porous templates.

3. Results and their discussion

3.1. Morphology, structure and composition

The study of the morphology and microstructure of various types of NWs using transmission electron microscopy (TEM) methods required additional sample preparation. It consisted in dissolving an aluminum oxide template containing arrays of nanowires in an aqueous solution of NaOH (6 M). The nanowires were then assembled using a neodymium magnet, washed in distilled water from an alkaline medium, and deposited on carbon-coated copper meshes. Figure 2 shows TEM images of NWs of various types. It can be seen that they are elongated cylindrical objects, however, nanowires of the B and C types have a branched structure at one end (there are smaller segments at the bottom of the pores compared to the main diameter of NW), which is due to the manufacturing features oxide patterns, namely, the presence of a stepwise stress reduction step, the use of which leads to pore branching. Since the time of electrolytic deposition was the same for all types of samples, the average length of the magnetic NW turned out to be close and amounted to $\sim 8-10\,\mu$m. The average diameter of the nanowires of type A, B, and C was $\sim 50-60$ nm.

The porosity of the synthesized samples, calculated according to the well-known formula for such structures [29,30]

$$p = \left(\frac{d}{D_{int}}\right)^2 \frac{2\sqrt{3}}{\pi},$$

where d is the diameter of the nanowires, D_{int} is the distance between the centers of the pores turned out to be equal to about 0.25 for all types of samples.

The presence of areas of different contrast in the TEM images of the Fe−Ni alloy nanowires indicates their polycrystalline structure. The transmission electron microscopy image analysis method was used to quantify the size of crystallites in synthesized nanowires. The essence of the method was to measure the linear volume occupied by individual crystallites on representative TEM images of each type of sample. Special attention was paid to estimating the proportion of large crystallites, defined as crystallites with a characteristic linear size of more than 30 nm. The analysis results showed that the samples of types A and B are characterized by a significant proportion of large crystallites, which in both cases is about 70 %. In contrast, a sample of the type C shows a smaller proportion of large crystallites, their contribution to the total linear volume is about 57 %. Differences in the size distribution of crystallites may be related to the peculiarities of obtaining different types of nanowires.

Electron diffraction pattern of the selected area (inset in Figure 2), showed that all types of NW from Fe−Ni alloy have a face-centered cubic lattice. For all types of samples, the crystal lattice parameter coincides within the error range and is 0.3529 ± 0.0008 nm, which is higher than the value of the lattice parameter for pure Ni equal to 0.3520 nm. This indicates that Fe atoms are embedded in the Ni crystal lattice and increase its size.

The composition was studied by energy dispersion microscopy using JEOL-2100 transmission electron microscope with the Bruker spectrometer option, the data are provided in Table 1.

The difference of the composition of samples of type A and B from samples of C type can be explained by the different potential of electrolytic deposition applied to them

Table 1. Composition of nanowire arrays of different types

Type	Fe, at.%	Ni, at.%
A	3.5	96.5
B	3	97
C	6.5	93.5

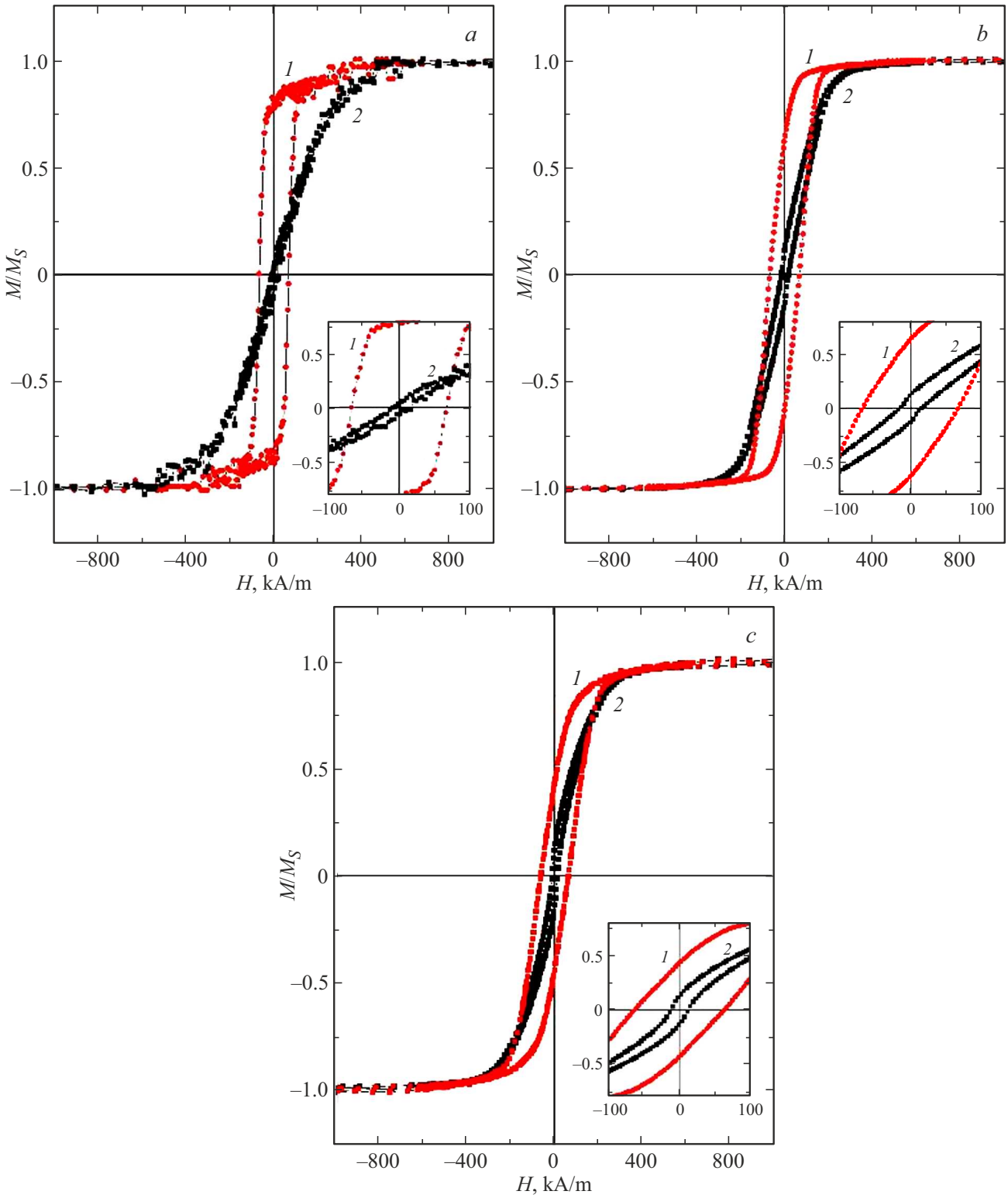

Figure 3. Hysteresis loops for nanowires arrays of type *A* (*a*), *B* (*b* and *C* (*c*), measured when the magnetic field is directed along the nanowire array (curve *1*) perpendicular (curve *2*), the graphs in the inserts are magnified.

Table 2. Magnetic characteristics of samples of types A, B and C

Type	H_C (∥), kA/m	H_C (⊥), kA/m	M/M_s (∥)	M/M_s (⊥)	M_s, kA/m
A	66.9	12.3	0.816	0.052	540
B	67.2	15.4	0.627	0.122	545
C	62.0	12.4	0.425	0.132	600

due to the peculiarities of manufacturing samples of this type.

3.2. Magnetic properties

Hysteresis loops measured on arrays of Fe−Ni alloy nanowires of different types are shown in Figure 3. The numerical values of the magnetic characteristics of each of the samples (coercive force when applying a magnetic field along and perpendicular to the axis of the nanowire array H_C (∥) and H_C (⊥), saturation magnetization M_s and residual magnetization M/M_s) are given in Table 2. It can be seen that all types of samples are characterized by pronounced magnetic anisotropy such as the axis of light magnetization parallel to the axis of the nanowire array, which indicates a significant contribution of the shape anisotropy to the effective anisotropy energy. A more detailed analysis of the hysteresis loops revealed some features of the magnetization reversal of arrays of nanowires of various types, which should be discussed in more detail. For instance, the hysteresis loop of a sample of type A, measured with the direction of the magnetic field perpendicular to the axis of the NWs array (Figure 3, *a*, curve *2*), has the lowest coercive force (according to Table 2) and reaches saturation in the largest field compared to the samples B and C.

The field required to achieve the orientation of the magnetization perpendicular to the axis of the nanowires of type A is about 278.5 kA/m, which is close to the value of $H_s = 2\pi M_s = 269.7$ kA/m (Table 2), which reflects the contribution of the shape anisotropy to the effective anisotropy sample [31]. Such an assessment for samples of the type B and C is impractical since they have significant heterogeneities in morphology.

It is worth noting that the hysteresis loop of a sample of type C, measured with the direction of the magnetic field perpendicular to the axis of the NWs array (see the box in Figure 3, *c*, curve *2*) shows an obvious bend in the region of small fields, which is significantly smaller for the type B sample (see the box in Figure 3, *b*, curve *2*) and is completely absent from the type sample A. The occurrence of this bend may be due to the presence of a magnetic phase, the magnetization of which lies at a certain angle relative to the axis of the NWs array. The most likely source of the inhomogeneous magnetic phase is a branched structure at the bottom of NWs arrays of types B and C, the presence of which leads to a local dispersion of magnetization and a complex distribution of its own demagnetizing field [31–33]. At the same time, type C samples are characterized by a more complex branched structure at the bottom of the pores, due to the thinning of the barrier layer, the minimum diameter of the segments of which (~ 18 nm) is smaller compared to samples of type B, in which the minimum diameter of the segments is ~ 26 nm. The magnitude of the residual magnetization decreases from samples of type A to samples of type C, which can also be explained by the presence of an inhomogeneous phase, which was discussed earlier.

3.3. Magnetoresistive properties

A study of the magnetoresistive properties of arrays of Fe−Ni alloy nanowires of various types has shown that they have the effect of magnetoresistance anisotropy. The normalized magnetoresistive hysteresis loops measured when an external magnetic field is applied perpendicular to the axis of an array of NWs of types A, B and C are shown in Figure 4. This figure also shows a magnetoresistive curve measured when an external magnetic field is applied along the axis of an array NWs of type B. The magnetoresistive curves for samples A and C are identical to the curve for sample B, so the corresponding data are not provided. The magnitude of the AMR effect was determined using the

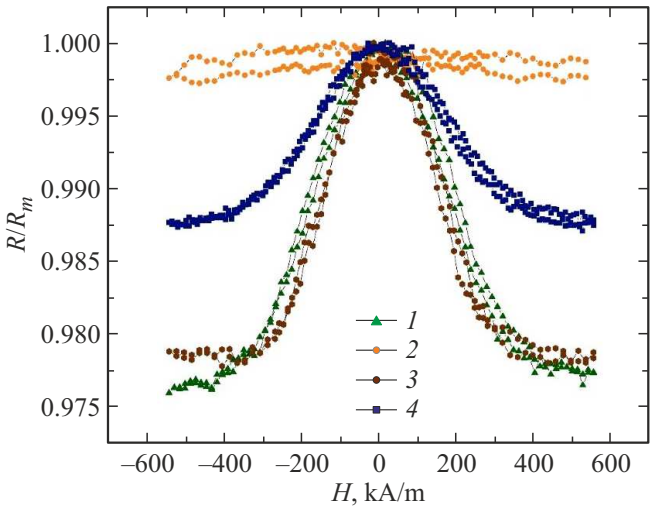

Figure 4. Dependence of electrical resistance on an external magnetic field applied perpendicular to the axis of the nanowire array for samples of the type A (curve *1*), B (curve *2*) and C (curve *3*), and along the axis of the nanowire array, for a sample type B (curve *4*).

following formula [34]:

$$\frac{\Delta R}{R} = \frac{R_{\parallel} - R_{\perp}}{\frac{1}{3} \cdot R_{\parallel} + \frac{2}{3} \cdot R_{\perp}},$$

where $R_{\parallel}$ and $R_{\perp}$ are the values of the electrical resistance of the samples when current flows parallel and perpendicular to the axis of the NWs array, respectively. The magnitude of the AMR effect was about 2.2 % for samples of the type *A* and *B*, which is slightly lower than the values typical for high-nickel alloys Fe−Ni (2.3−4 % [35–37]). The reduced level of AMR in our case may be associated with significant surface scattering of conduction electrons in NWs [35,36]. The magnitude of the AMR effect was even lower for type *C* samples (1.3,%). In this case, an additional contribution to the scattering of conduction electrons is probably attributable to the increased density of the intergranular boundaries [36–40], since this type of sample, according to TEM microscopy, is characterized by a smaller average crystallite size.

4. Conclusion

A synthesis was performed and a comprehensive study of arrays of Fe−Ni alloy nanowires of three different types, differing in morphology and microstructure. Among other things, conditions have been established for obtaining porous aluminum oxide matrices with branches in the bottom, which enhance the dispersion of the polycrystalline microstructure of NWs and are responsible for the formation of a magnetic phase in them with a magnetization of the non-collinear axis of the main NWs array.

An effective technique for creating conductive layers on the surfaces of NWs arrays has been proposed, which made it possible to conduct an adequate analysis of their magnetoresistive properties. Among other things, the presence of all types of magnetoresistance anisotropy effect in NWs, the magnitude of which is maximum (2.3,%) in samples that do not contain branching elements.

Funding

The research was supported by a grant from the Russian Science Foundation No. 25-22-00240, https://rscf.ru/project/25-22-00240/.

Conflict of interest

The authors declare that they have no conflict of interest.

References

[1] J.M.D. Coey. Magnetism and magnetic materials. Cambridge university press, NY (2010).
[2] M. Vazquez. J. Magn. Magn. Mater. **543**, 168634 (2022).
[3] J. Um, Y. Zhang, W. Zhou, M.R. Zamani Kouhpanji, C. Radu, R.R. Franklin, B.J. Stadler. ACS Appl. Nano Mater. **4**, *4*, 3557 (2021).
[4] J.A. Moreno, C. Bran, M. Vazquez, J. Kosel. IEEE Trans. Magn. **57**, *4*, 1 (2021).
[5] L. Piraux. Appl. Sci. **10**, *5*, 1832 (2020).
[6] .A. Fernandez-Roldan, R.P. del Real, C. Bran, M. Vazquez, O. Chubykalo-Fesenko. Phys. Rev. B **102**, *2*, 024421 (2020).
[7] W. Lee, S.-J. Park. Chem. Rev. **114**, *15*, 7487 (2014).
[8] A. Vorobjova, D. Tishkevich, D. Shimanovich, T. Zubar, K. Astapovich, A. Kozlovskiy, A. Trukhanov. RSC Adv. **11**, *7*, 3952 (2021).
[9] D. Kelly, J.E. Wegrowe, T.K. Truong, X. Hoffer, J.P. Ansermet. Phys. Rev. B **68**, *13*, 134425 (2003).
[10] M. Hayashi, L. Thomas, R. Moriya, C. Rettner, S.S. Parkin. Science, **320**, 5873, 209−211 (2008).
[11] J.A. Fernandez-Roldan, O. Chubykalo-Fesenko. APL Mater. **10**, 11 (2022).
[12] C. Bran, J.A. Fernández-Roldán, J.A. Moreno, A.F. Rodríguez, R.P. del Real, A. Asenjo, O. Chubykalo-Fesenko. Nanoscale **15**, *18*, 8387 (2023).
[13] J. Hurst, A. De Riz, M. Staňo, J.C. Toussaint, O. Fruchart, D. Gusakova. Phys. Rev. B **103**, *2*, 024434 (2021).
[14] J.A. Moreno, J. Kosel. Sci. Rep. **12**, *1*, 19510 (2022).
[15] D. Bhattacharya, Z. Chen, C.J. Jensen, C. Liu, E.C. Burks, D.A. Gilbert, K. Liu. Nano Lett. **22**, *24*, 10010 (2022).
[16] B. Chen, M. Zeng, K.H. Khoo, D. Das, X. Fong, S. Fukami, S. Ter Lim. Mater. Today **70**, 193 (2023).
[17] J. Zeng, Y. Chen, J. Liu, T. Xu, L. Fang, Y. Guo. ACS Appl. Mater. Interfaces **16**, *43*, 59088 (2024).
[18] G. Hrkac, J. Dean, D.A. Allwood. Philos. Trans. R. Soc. A **369**, *1948*, 3214 (2011).
[19] Y. Rheem, B.Y. Yoo, W.P. Beyermann, N.V. Myung. Nanotechnology **18**, *1*, 015202 (2006).
[20] S.N. Kozlov, O.V. Skryabina, S.V. Egorov, I.A. Golovchanskiy, A.A. Klimenko, K.S. Napolskii, V.S. Stolyarov. J. Appl. Phys. **125**, 6 (2019).
[21] S. Pignard, G. Goglio, A. Radulescu, L. Piraux, S. Dubois, A. Declemy, J.L. Duvail. J. Appl. Phys. **87**, *2*, 824 (2000).
[22] J.E. Wegrowe, D. Kelly, A. Franck, S.E. Gilbert, J.P. Ansermet. Phys. Rev. Lett. **82**, *18*, 3681 (1999).
[23] Huang, L. Li, X. Luo, Zhu, Li. J. Phys. Chem. C **112**, *5*, 1468 (2008).
[24] M.I. Sobirov, A.Y. Samardak, S.A. Satsuk, K.A. Rogachev, N.A. Ognev, G.A. Leyko, A.S. Samardak. J. Supercond. Nov. Magn. **38**, *1*, 1 (2025).
[25] B. Lakshmi, C. Patrissi, C. Martin. Chem. Mater. **9**, 2544 (1997).
[26] Y. Zhang, G. Li, Y. Wu, B. Zhang, W. Song, L. Zhang. Adv. Mater. **14**, *17*, 1227 (2002).
[27] E.L.T. França, A.R. Santos, L.K.C.S. Assis, S. Castro-Lopes, D.M. Oliveira, A.S.D. Carvalho, E.P. Hernández. J. Magn. Magn. Mater. **605**, 172310 (2024).
[28] A.I. Vorobyeva, E.A. Utkina, O.M. Komar. Mikroelektronika **42**, *2*, 105 (2013). (in Russian).
[29] V. Vega, V.M. Prida, J.A. García, M. Vazquez. Phys. Status Solidi A, **208**, *3*, 553 (2011).
[30] A.S. Samardak, F. Nasirpouri, M. Nadi, E.V. Sukovatitsina, A.V. Ognev, L.A. Chebotkevich, S.V. Komogortsev. J. Magn. Magn. Mater. **383**, 94 (2015).
[31] L. Sun, Y. Hao, C.L. Chien, P.C. Searson. IBM J. Res. Dev. **49**, *1*, 79 (2005).

[32] A.E. Dryagina, A.N. Gorkovenko, N.A. Kulesh, E.V. Kudyukov, A.V. Viblaya, A.A. Yushkov, A.A. Veryasova, V.I. Pastukhov, A.S. Kalashnikova, V.O. Vaskovsky. FMM **125**, *4*, 413 (2024). (in Russian).
[33] E.A. Denisova, L.A. Chekanova, S.V. Komogortsev, R.S. Iskhakov, I.G. Vazhenina, I.V. Nemtsev, O.A. Li. Izv. RAN. Ser. Fiz. **88**, *4*, 618 (2024). (in Russian).
[34] H. Corte-León, V. Nabaei, A. Manzin, J. Fletcher, P. Krzysteczko, H.W. Schumacher, O. Kazakova. Sci. Rep. **4**, *1*, 6045 (2014).
[35] T. McGuire, R.L. Potter. IEEE Trans. Magn. **11**, *4*, 1018 (1975)
[36] R.M. Bozorth. Phys. Rev. **70**, *11–12*, 923 (1946).
[37] M. Bolte, M. Steiner, C. Pels, M. Barthelmess, J. Kruse, U. Merkt, D. Pfannkuche. Phys. Rev. B **72**, *22*, 224436 (2005).
[38] J. Kondo. Prog. Theor. Phys. **27**, *4*, 772 (1962).
[39] M. Chakravorty, A.K. Raychaudhuri. J. Appl. Phys. **117**, 3 (2015).
[40] N. Djuzhev, A. Iurov, N. Mazurkin, M. Chinenkov, A. Trifonov, M. Pushkina. EPJ Web Conf. **185**, 01003 (2018).

Translated by A.Akhtyamov